REVIEW AND SUMMARY

This chapter was devoted to the analysis and design of *shafts* subjected to twisting couples, or *torques*. Except for the last two sections of the chapter, our discussion was limited to *circular shafts*.

Deformations in circular shafts

In a preliminary discussion [Sec. 3.2], it was pointed out that the distribution of stresses in the cross section of a circular shaft is *statically indeterminate*. The determination of these stresses, therefore, requires a prior analysis of the *deformations* occurring in the shaft [Sec. 3.3]. Having demonstrated that in a circular shaft subjected to torsion, *every cross section remains plane and undistorted,* we derived the following expression for the *shearing strain* in a small element with sides parallel and perpendicular to the axis of the shaft and at a distance ρ from that axis:

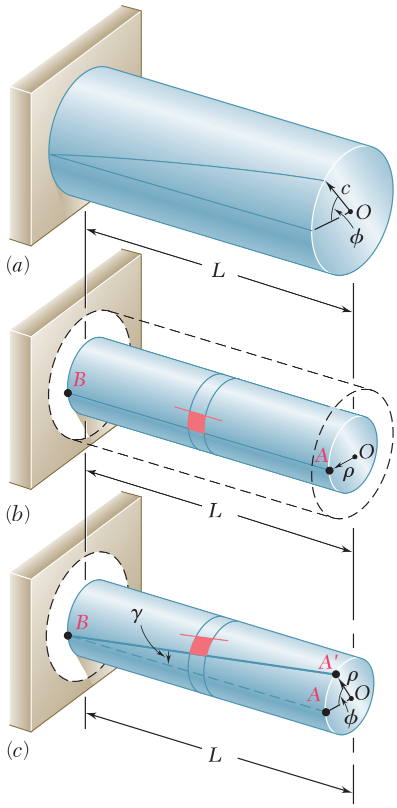

Fig. 3.57

$$\gamma = \frac{\rho\phi}{L} \tag{3.2}$$

where ϕ is the angle of twist for a length L of the shaft (Fig. 3.57). Equation (3.2) shows that the *shearing strain in a circular shaft varies linearly with the distance from the axis of the shaft.* It follows that the strain is maximum at the surface of the shaft, where ρ is equal to the radius c of the shaft. We wrote

$$\gamma_{\max} = \frac{c\phi}{L} \qquad \gamma = \frac{\rho}{c}\gamma_{\max} \tag{3.3, 4}$$

Shearing stresses in elastic range

Considering *shearing stresses* in a circular shaft within the elastic range [Sec. 3.4] and recalling Hooke's law for shearing stress and strain, $\tau = G\gamma$, we derived the relation

$$\tau = \frac{\rho}{c}\tau_{\max} \tag{3.6}$$

which shows that within the elastic range, the *shearing stress τ in a circular shaft also varies linearly with the distance from the axis of the shaft.* Equating the sum of the moments of the elementary forces exerted on any section of the shaft to the magnitude T of the torque applied to the shaft, we derived the *elastic torsion formulas*

$$\tau_{\max} = \frac{Tc}{J} \qquad \tau = \frac{T\rho}{J} \tag{3.9, 10}$$

where c is the radius of the cross section and J its centroidal polar moment of inertia. We noted that $J = \frac{1}{2}\pi c^4$ for a solid shaft and $J = \frac{1}{2}\pi(c_2^4 - c_1^4)$ for a hollow shaft of inner radius c_1 and outer radius c_2.

We noted that while the element a in Fig. 3.58 is in pure shear, the element c in the same figure is subjected to normal stresses of the same magnitude, Tc/J, two of the normal stresses being tensile and two compressive. This explains why in a torsion test ductile materials, which generally fail in shear, will break along a plane perpendicular to the axis of the specimen, while brittle materials, which are weaker in tension than in shear, will break along surfaces forming a 45° angle with that axis.

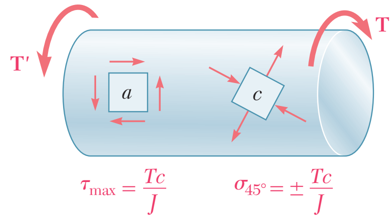

Fig. 3.58

Angle of twist

In Sec. 3.5, we found that within the elastic range, the angle of twist ϕ of a circular shaft is proportional to the torque T applied to it (Fig. 3.59). Expressing ϕ in *radians*, we wrote

$$\phi = \frac{TL}{JG} \tag{3.16}$$

where L = length of shaft
J = polar moment of inertia of cross section
G = modulus of rigidity of material

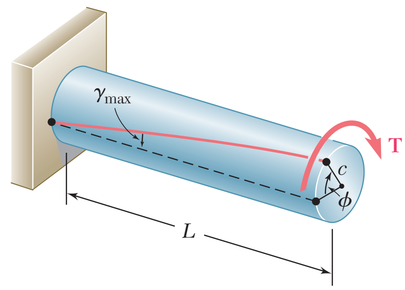

Fig. 3.59

If the shaft is subjected to torques at locations other than its ends or consists of several parts of various cross sections and possibly of different materials, the angle of twist of the shaft must be expressed as the *algebraic sum* of the angles of twist of its component parts [Sample Prob. 3.3]:

$$\phi = \sum_i \frac{T_i L_i}{J_i G_i} \tag{3.17}$$

We observed that when both ends of a shaft BE rotate (Fig. 3.60), the angle of twist of the shaft is equal to the *difference* between the angles of rotation ϕ_B and ϕ_E of its ends. We also noted that when two shafts AD and BE are connected by gears A and B, the torques applied, respectively, by gear A on shaft AD and by gear B on shaft BE are *directly proportional* to the radii r_A and r_B of the two gears—since the forces applied on each other by the gear teeth at C are equal and opposite. On the other hand, the angles ϕ_A and ϕ_B through which the two gears rotate are *inversely proportional* to r_A and r_B—since the arcs CC' and CC'' described by the gear teeth are equal [Example 3.04 and Sample Prob. 3.4].

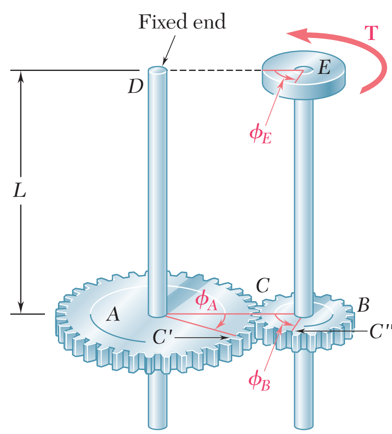

Fig. 3.60

Statically indeterminate shafts

If the reactions at the supports of a shaft or the internal torques cannot be determined from statics alone, the shaft is said to be *statically indeterminate* [Sec. 3.6]. The equilibrium equations obtained from free-body diagrams must then be complemented by relations involving the deformations of the shaft and obtained from the geometry of the problem [Example 3.05, Sample Prob. 3.5].

Transmission shafts

In Sec. 3.7, we discussed the *design of transmission shafts.* We first observed that the power P transmitted by a shaft is

$$P = 2\pi f T \tag{3.20}$$

where T is the torque exerted at each end of the shaft and f the *frequency* or speed of rotation of the shaft. The unit of frequency is the revolution per second (s^{-1}) or *hertz* (Hz). If SI units are used, T is expressed in newton-meters (N · m) and P in *watts* (W). If U.S. customary units are used, T is expressed in lb · ft or lb · in., and P in ft · lb/s or in · lb/s; the power may then be converted into *horsepower* (hp) through the use of the relation

$$1 \text{ hp} = 550 \text{ ft} \cdot \text{lb/s} = 6600 \text{ in} \cdot \text{lb/s}$$

To design a shaft to transmit a given power P at a frequency f, you should first solve Eq. (3.20) for T. Carrying this value and the maximum allowable value of τ for the material used into the elastic formula (3.9), you will obtain the corresponding value of the parameter J/c, from which the required diameter of the shaft may be calculated [Examples 3.06 and 3.07].

Stress concentrations

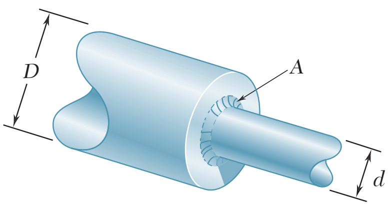

Fig. 3.61

In Sec. 3.8, we discussed *stress concentrations* in circular shafts. We saw that the stress concentrations resulting from an abrupt change in the diameter of a shaft can be reduced through the use of a *fillet* (Fig. 3.61). The maximum value of the shearing stress at the fillet is

$$\tau_{\max} = K\frac{Tc}{J} \tag{3.25}$$

where the stress Tc/J is computed for the smaller-diameter shaft, and where K is a stress-concentration factor. Values of K were plotted in Fig. 3.29 on p. 179 against the ratio r/d, where r is the radius of the fillet, for various values of D/d.

Plastic deformations

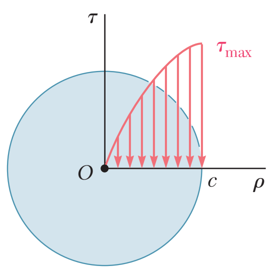

Fig. 3.62

Sections 3.9 through 3.11 were devoted to the discussion of *plastic deformations* and *residual stresses* in circular shafts. We first recalled that even when Hooke's law does not apply, the distribution of *strains* in a circular shaft is always linear [Sec. 3.9]. If the shearing-stress-strain diagram for the material is known, it is then possible to plot the shearing stress τ against the distance ρ from the axis of the shaft for any given value of $\tau_{\max}$ (Fig. 3.62). Summing the contributions to the torque of annular elements of radius ρ and thickness $d\rho$, we expressed the torque T as

$$T = \int_0^c \rho\tau(2\pi\rho\, d\rho) = 2\pi \int_0^c \rho^2\tau\, d\rho \tag{3.26}$$

where τ is the function of ρ plotted in Fig. 3.62.

Modulus of rupture

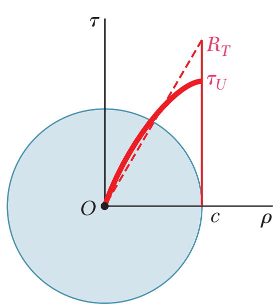

Fig. 3.63

An important value of the torque is the ultimate torque T_U which causes failure of the shaft. This value can be determined, either experimentally, or by carrying out the computations indicated above with $\tau_{\max}$ chosen equal to the ultimate shearing stress τ_U of the material. From T_U, and assuming a linear stress distribution (Fig 3.63), we determined the corresponding fictitious stress $R_T = T_U c/J$, known as the *modulus of rupture in torsion* of the given material.

Considering the idealized case of a *solid circular shaft* made of an *elastoplastic material* [Sec. 3.10], we first noted that, as long as

τ_{max} does not exceed the yield strength τ_Y of the material, the stress distribution across a section of the shaft is linear (Fig. 3.64*a*). The torque T_Y corresponding to $\tau_{max} = \tau_Y$ (Fig. 3.64*b*) is known as the *maximum elastic torque;* for a solid circular shaft of radius c, we have

$$T_Y = \tfrac{1}{2}\pi c^3 \tau_Y \tag{3.29}$$

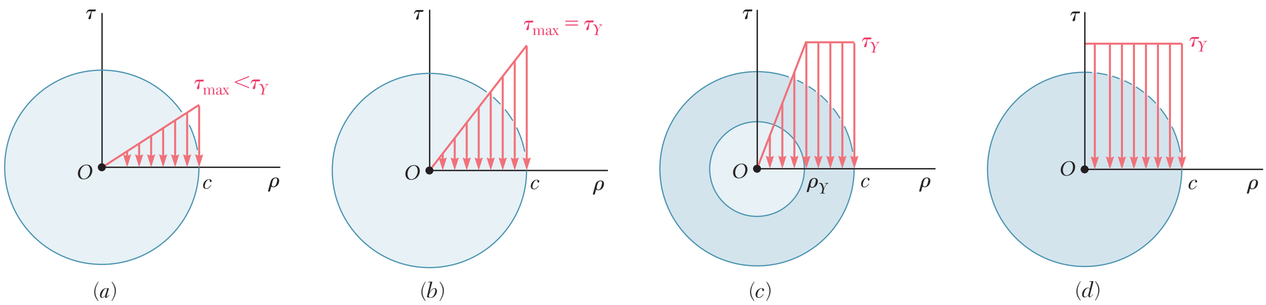

Fig. 3.64

Solid shaft of elastoplastic material

As the torque increases, a plastic region develops in the shaft around an elastic core of radius ρ_Y. The torque T corresponding to a given value of ρ_Y was found to be

$$T = \frac{4}{3}T_Y\left(1 - \frac{1}{4}\frac{\rho_Y^3}{c^3}\right) \tag{3.32}$$

We noted that as ρ_Y approaches zero, the torque approaches a limiting value T_p, called the *plastic torque* of the shaft considered:

$$T_p = \frac{4}{3}T_Y \tag{3.33}$$

Plotting the torque T against the angle of twist ϕ of a solid circular shaft (Fig. 3.65), we obtained the segment of straight line $0Y$ defined by Eq. (3.16), followed by a curve approaching the straight line $T = T_p$ and defined by the equation

$$T = \frac{4}{3}T_Y\left(1 - \frac{1}{4}\frac{\phi_Y^3}{\phi^3}\right) \tag{3.37}$$

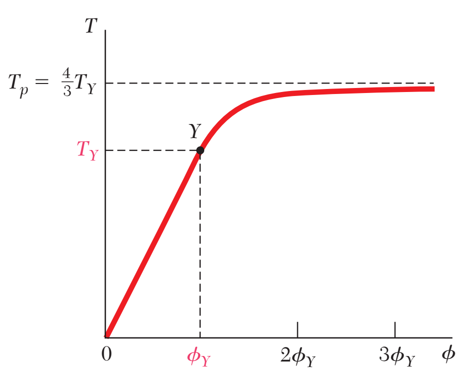

Fig. 3.65

Permanent deformation. Residual stresses

Loading a circular shaft beyond the onset of yield and unloading it [Sec. 3.11] results in a *permanent deformation* characterized by the angle of twist $\phi_p = \phi - \phi'$, where ϕ corresponds to the loading phase described in the previous paragraph, and ϕ' to the unloading phase represented by a straight line in Fig. 3.66. There will also be *residual stresses* in the shaft, which can be determined by adding the maximum stresses reached during the loading phase and the reverse stresses corresponding to the unloading phase [Example 3.09].

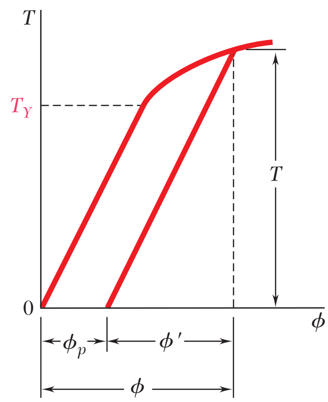

Fig. 3.66

Torsion of noncircular members

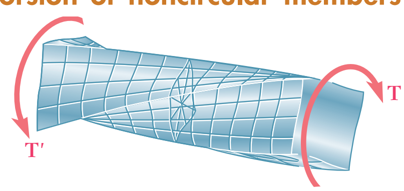

Fig. 3.67

The last two sections of the chapter dealt with the torsion of *noncircular members.* We first recalled that the derivation of the formulas for the distribution of strain and stress in circular shafts was based on the fact that due to the axisymmetry of these members, cross sections remain plane and undistorted. Since this property does not hold for noncircular members, such as the square bar of Fig. 3.67, none of the formulas derived earlier can be used in their analysis [Sec. 3.12].

Bars of rectangular cross section

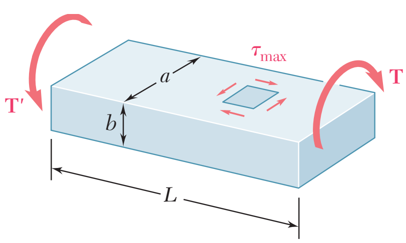

Fig. 3.68

It was indicated in Sec. 3.12 that in the case of straight bars with a *uniform rectangular cross section* (Fig. 3.68), the maximum shearing stress occurs along the center line of the *wider* face of the bar. Formulas for the maximum shearing stress and the angle of twist were given without proof. The *membrane analogy* for visualizing the distribution of stresses in a noncircular member was also discussed.

Thin-walled hollow shafts

We next analyzed the distribution of stresses in *noncircular thin-walled hollow shafts* [Sec. 3.13]. We saw that the shearing stress is parallel to the wall surface and varies both across the wall and along the wall cross section. Denoting by τ the average value of the shearing stress computed across the wall at a given point of the cross section, and by t the thickness of the wall at that point (Fig. 3.69), we showed that the product $q = \tau t$, called the *shear flow,* is constant along the cross section.

Furthermore, denoting by T the torque applied to the hollow shaft and by $\mathcal{A}$ the area bounded by the center line of the wall cross section, we expressed as follows the average shearing stress τ at any given point of the cross section:

$$\tau = \frac{T}{2t\mathcal{A}} \qquad (3.53)$$

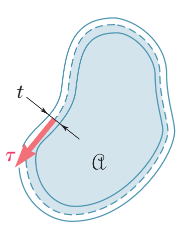

Fig. 3.69